

A Long-Term Voltage Stability Margin Index Based on Multiple Real Power Flow Solutions

Bin Wang[†], Senior Member, IEEE, Dan Wu[‡], Member, IEEE, Xiaowen Su[†],
Kai Sun^{*}, Senior Member, IEEE, and Le Xie^{**}, Fellow, IEEE

Abstract—In this paper, we demonstrate the distribution of real-valued power flow solutions and its application to the long-term voltage stability. It is the first time in power engineering we realize that even a small-scale IEEE standard power system can admit a humongous number of real-valued solutions for a single load and generation profile. For example, the IEEE 30-bus system can achieve 25686 many different real-valued solutions at a light loading condition. Furthermore, a mysterious class of “false” power flow solutions is reported and analyzed rigorously as legitimate numerical solutions. All solution sets investigated in this paper are posted online associated with this paper to support potential future applications [1]. Based on these extensive solved power flow solutions, we exhibit their occurrence patterns and distributions at different loading levels, and propose a long-term voltage stability margin index to quantify the long-term voltage stability of a given power flow condition. Numerical studies on a 5-bus system and a 57-bus system show the feasibility and effectiveness of the proposed index in assessing power system long-term voltage stability margin.

Index Terms—Multiple power flow solutions, holomorphic embedding based continuation, “short circuit” solution, distribution pattern, long-term voltage stability

I. INTRODUCTION

The increasing integration of distributed energy resources and demand responses provides great flexibility to operate power grids in a more efficient manner. However, this flexibility can also alter the traditional load pattern and increase the pattern diversity [2], creating a challenge for power grid planning and operation—keeping power flow balanced between generation and load at all time scales.

Power balance equations (power flow equations) are used in daily grid planning and operation to define and evaluate the grid operating condition. Power balance equations can admit multiple real solutions. The one that the grid is operated at is usually called the high-voltage solution since the dynamic power system is stable at this solution where all bus voltages are close to one per unit. Other than the high-voltage solution, most of the rest do not allow a stable and secure operation. Still, their locations and distributions convey important information about the underlying system, shown to be useful for

both static and dynamical stability analysis [3], [4]. Finding multiple real power flow solutions is not a trivial task. It was computationally tractable only up to systems with 14 buses [5]. A recently developed technique, called *holomorphic embedding based continuation* (HEBC) method [6], pushes this boundary to medium-sized systems. Although there is still a lack of theoretical proof to show whether the HEBC method can find all real power flow solutions, in all verifiable cases [6] HEBC method always gives complete solution sets. To assess potential statistical properties of power flow solutions, a few cases, i.e., IEEE 14, 30, 39 and 57 bus systems, are adopted for a comprehensive investigation. Their solution sets are posted online at [1] for any potential interests of research.

Among different potential applications of multiple real power flow solutions, this paper focuses on the long-term voltage stability problem and proposes a stability margin index. The commonly used voltage stability margin is defined in the power space between the current operating condition and the nose point, given a specific stressing direction to increase the load and generation. Other existing voltage stability margin indices in the literature usually rely on simplifying assumptions on power flow equations [7], leading to potential inaccuracies and errors. In this paper, we explore a minimum distance in the voltage space between the high-voltage solution, i.e., the current operating condition, and all other real power flow solutions to the same power balance equations. Without recent advances in HEBC [6], previous work [8], [9] can only exploit a nearby low-voltage power flow solution, which, in theory, has not been proved to be the “closest” low-voltage solution. Here we inherit a similar idea with a complete and more comprehensive study of real power flow solutions. Compared to existing voltage stability margin indices, the proposed index is free of any pre-defined stressing directions, making it a global index. In addition, the proposed index does not require any simplifying assumptions on power flow equations. Still, a detailed investigation to compare with other indices in terms of accuracy, computational complexity, and scalability is needed and will be part of our future work.

The rest of the paper is organized in the following way: Section II introduces a class of power flow solutions, named “short circuit” solutions, that satisfy the power balance equations but are not meaningful. Section III illustrates the number of power flow solutions and their distributions. Section IV presents the proposed voltage stability margin index and its application. Section V gives the conclusion.

[†]: Department of Electrical and Computer Engineering, University of Texas at San Antonio, San Antonio, TX, {bin.wang2, xiaowen.su}@utsa.edu;
[‡]: School of Electrical and Electronic Engineering, Huazhong University of Science and Technology, Lab for Information and Decision Systems, Massachusetts Institute of Technology, Cambridge, MA, danwumit@mit.edu;
^{*}: Department of Electrical Engineering and Computer Science, University of Tennessee, TN, kaisun@utk.edu; ^{**}: Department of Electrical and Computer Engineering, Texas A&M University, College Station, TX, le.xie@tamu.edu

II. “SHORT CIRCUIT” SOLUTIONS

A specific type of power flow solutions is observed. These particular solutions satisfy the power balance equations, namely the power injection model, and thus are the solutions to the power flow problem. But they do not satisfy the Kirchhoff’s Current Law (KCL) as explained in the following. We refer to them as the “short circuit” solutions. A necessary condition for the existence of “short circuit” solution is that: *a power grid has at least one transit-bus which is a special PQ-bus with zero nodal power injection.*

Consider the power balance equation at node- i ,

$$V_i \times I_i^* = P_i + jQ_i \quad (1)$$

where $V_i \in \mathbb{C}$ is the complex voltage at node- i , $I_i^* \in \mathbb{C}$ is the conjugate of complex current at node- i , $P_i + jQ_i \in \mathbb{C}$ is the complex power injection at node- i .

If node- i is a transit-bus, then $P_i + jQ_i = 0$, which suggests that either $V_i = 0$ or $I_i = 0$ ¹. When $V_i = 0$ and $I_i \neq 0$, an external current I_i is supposed to enter node- i from somewhere. Since $V_i = 0$ at this point, the solution suggests that the system is grounded at node- i . However, the system is not physically connected to the ground at node- i . Therefore, KCL fails at this solution. One can interpret this “short circuit” solution as a feasible solution to the grounded power flow problem at node- i . Reference [10] reported a numerical problem caused by “short circuit” solutions, i.e. voltage can be wrongly trapped at zero after clearing a short-circuit fault, when using power injection model in dynamic simulations.

Our studies show that “short circuit” solutions are more likely to happen at a lighter loading level. For example, Fig. 1 shows the number of “short circuit” solutions with respect to the load scaling factor². When the load increases to a certain level, they eventually disappear. But at low loading levels, the number of “short circuit” solutions can be huge. For instance, in Fig. 1(a), Case30 has at least 6849 “short circuit” solutions at 10% loading level. A light loading level usually admits much more “short circuit” solutions because the constant loading line can intersect with many PV (QV) branches for the grounded power flow problem.

“Short circuit” solutions can also occur when constant impedance loads exist. These load nodes are transit-bus, and thus can admit many such solutions at a light loading level.

A simple way to avoid “short circuit” solutions is to add a small power injection, say, $10^{-5} p.u.$ ³, at each transit-bus. As long as the power injection at each node- i in (1) is non-zero, neither V_i nor I_i is zero.

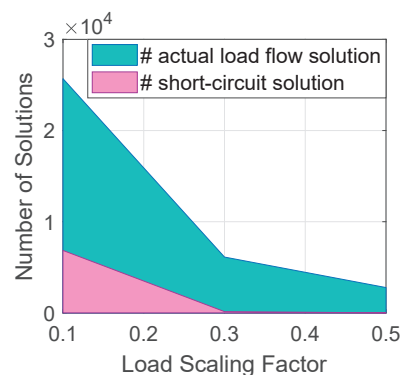
III. NUMERICAL STUDY OF SOLUTION DISTRIBUTION

This section first illustrates that the number of power flow solutions decreases with the increase of loading level. It is

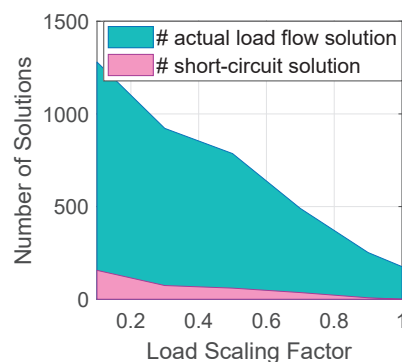
¹It is possible that both V_i and I_i vanish to zero. However, this is rather rare and hasn’t been observed in our studies.

²The load scaling factor scales every complex-valued load in the system.

³In our simulations the power mismatch error is below 10^{-9} p.u. Hence a 10^{-5} power injection will not be confused by the error threshold.



(a) Case30



(b) Case39

Fig. 1: Number of Short-Circuit Solutions

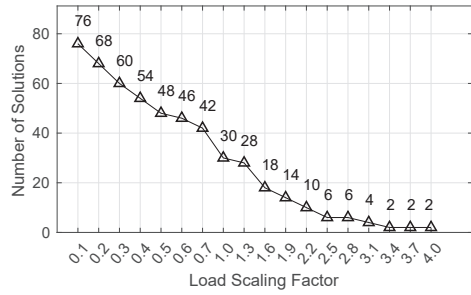
then shown that under lightly-loaded conditions, the identified solutions in each case are not randomly distributed, but exhibit distinct patterns. A scrutiny on the identified solution sets in terms of voltage magnitudes of PQ buses and reactive power of PV buses is presented.

A. Number of Solutions at Different Loading Levels

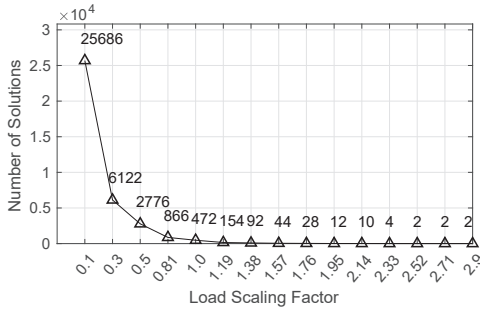
It is expected that as the loading level increases, the number of power flow solutions decreases, e.g. down to two solutions right before the voltage collapse at the saddle node as illustrated in Fig. 2. On the other hand, at light loading levels, the number of solutions can be very huge. For instance, Fig. 2(b) shows that 10% loading induces at least 25686 power flow solutions for Case30. This huge number, probably even greater for lighter loading or larger cases, makes it very challenging and less attractive to find all associated power flow solutions because the system stability is usually of less a concern under light loading conditions. At extremely heavy loading conditions, however, the number of solutions can be very small. Therefore, it is more practical and beneficial to identify these solutions for stressed power systems.

B. Node Voltage Pattern

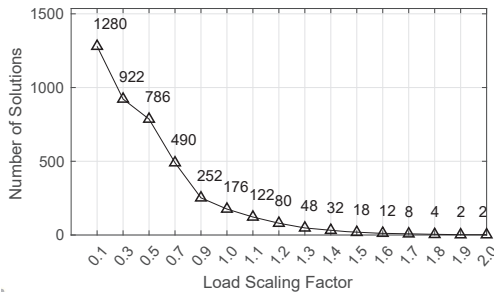
An interesting observation is that for each test case the nodes can be clustered by a few special voltage patterns. For example, Fig. 3 depicts four basic patterns that occur



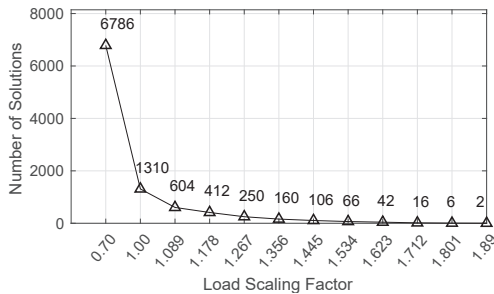
(a) Case14



(b) Case30



(c) Case39



(d) Case57

Fig. 2: Number of power flow solutions as loading level increases

in Case30, where each dot represents a voltage solution. The horizontal and vertical axes respectively represent the real and imaginary parts of the complex voltage. Table I summarizes the clusters of nodes that exhibit similar patterns as shown in Fig. 3. These structures persist as the loading condition changes. A light loading level, i.e. 10%, is adopted here since it gives a sufficient number of power flow solutions for

exhibiting potential statistical properties. A common pattern omitted here is a fixed-radius circle which is associated with each PV bus.

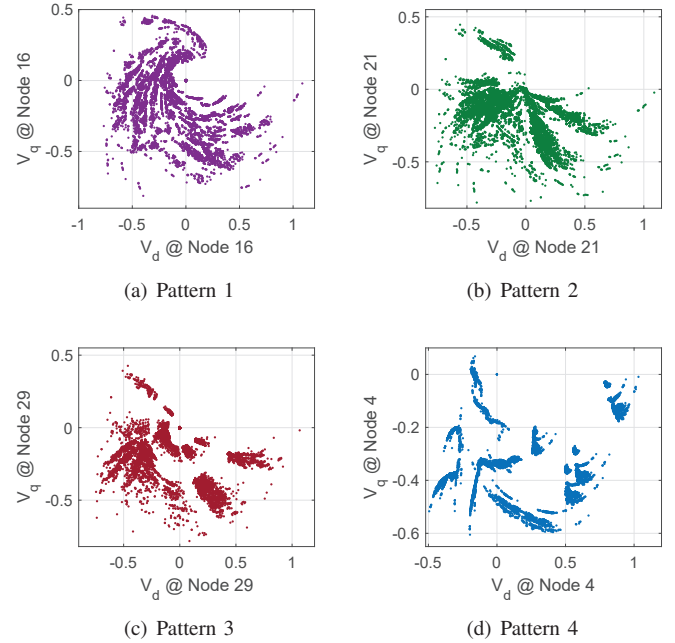


Fig. 3: Voltage Patterns for Case30 at 10% Load (25686 Solutions)

TABLE I: Bus Grouping by Voltage Pattern of Case30

Patterns	1	2	3	4
Buses	12, 14-16	17-24	9,10,25-27,29,30	3,4,6,7,28

The 39-bus system and the 57-bus system also exhibit a few distinctive voltage patterns. Usually, adjacent nodes are more likely to share the same pattern, but it is not always the case. Whether different patterns reveal local structural properties of the system is an open question. But the persistence of these patterns under different loading conditions may suggest a relation with the network topology. Some of the patterns are further depicted in Subsection-D with engineering limit considerations.

To reveal the statistical characteristics of power flow solutions, we discretized the voltage magnitude range $[0, 1.1]$ p.u. for 100 even intervals, and count the number of solutions for each interval. Sample distributions are depicted in Fig. 4, which exhibits persisting patterns that are consistent with the observations in Fig. 3.

IV. A LONG-TERM VOLTAGE STABILITY MARGIN INDEX

With the multiple real power flow solutions calculated by the HEBC method, this section presents one application of these power flow solutions on power system long-term voltage stability assessment. Specifically, a stability margin index of a N -bus system at a given load level P_L is defined as follows:

$$m = \min_j (||V_H - V_{L,j}||) \quad (2)$$

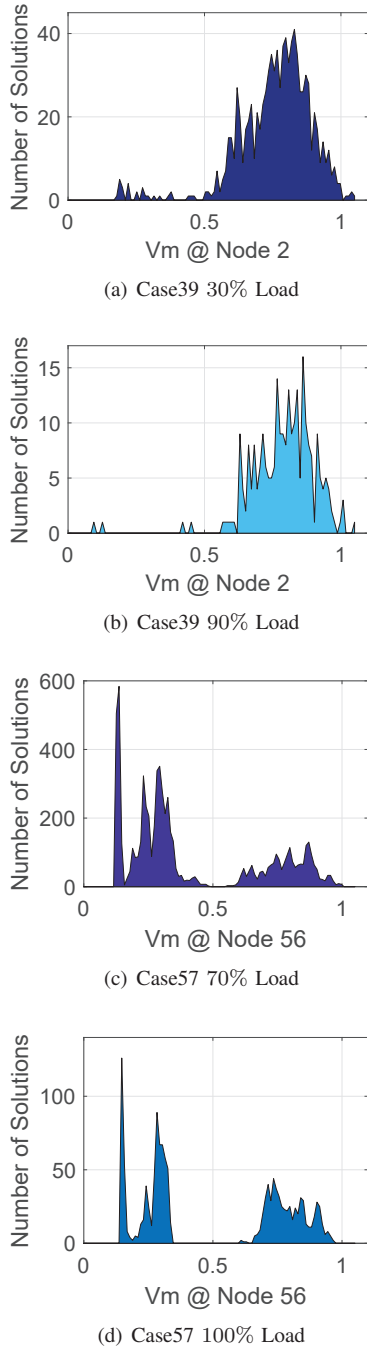


Fig. 4: Voltage Magnitude Distributions

where $V_H \in \mathbb{C}^N$ is the only high voltage solution and $V_{L,j} \in \mathbb{C}^N$, $j \in \{1, 2, \dots, n\}$, are n low-voltage solutions. m is the proposed voltage stability margin index, and P_L represents the system total active load.

The conceptual interpretation of the proposed voltage stability margin index is presented in Sub-section A and the numerical experiments are shown in Sub-section B.

A. Conceptual Interpretation of the Proposed Voltage Stability Margin Index on a Two-bus System

Figure 5 shows a typical P-V curve from a two-bus system with a constant power load connected to an infinite bus through a line. All power flow solutions in the two-bus system are illustrated, and the popular voltage stability margin index defined by the distance between the nose point and the current loading condition is discussed. Note that the definition of this stability margin relies on the choice of stressing direction, i.e., which and how loads and generations are increased. Then, the proposed voltage stability margin index is illustrated and interpreted on the P-V curve. In contrast, the proposed voltage stability margin index is a characterization of the given power flow steady state, completely independent of any specific stressing direction of generations and loads. This could be particularly useful when power flow patterns change more significantly and more frequently, such that defining very few typical stressing directions, as used by today's practice for evaluation, is challenging. This could be true especially for modern and future power grids dominated by massive intermittent and undispachable renewables.

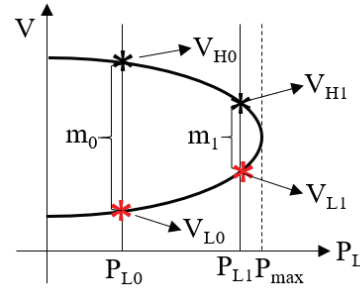


Fig. 5: Illustration on voltage stability margin on P-V curve

Specifically, the proposed voltage stability margin index at a given load level P_{L0} is defined as the distance between the high-voltage solution V_{H0} and the only low-voltage solution V_{L0} and is denoted as m_0 . As the system increases its loading condition from P_{L0} and P_{L1} , the margin index decreases from m_0 to m_1 . In a general large-scale power system, we assume that there is only one high-voltage solution in the system and all other solutions are low-voltage solutions. Therefore, the proposed voltage stability margin index is the minimum distance in voltage space between the high-voltage solution and all other real power flow solutions to the same power balance equations. Note that the proposed voltage stability margin index does not rely on knowing the nose point in a specified stressing direction, instead, it only depends on the global properties of power balance equations, i.e., the real solutions at the given load level.

B. Numerical Studies on 5-Bus and 57-Bus Test Systems

Numerical studies are conducted on two cases, i.e., a 5-bus system and a 57-bus system, to demonstrate how the proposed voltage stability margin index characterizes the distance between the current operating condition to the voltage stability

limit. The results are plotted as shown in Fig. 6. The horizontal axis is the load scaling factor. Default loading conditions with a load scaling factor of 1.0 in the two systems are 170 MVA and 1295 MVA, respectively. The vertical axis is the proposed stability margin index. For the 5-bus system (or the 57-bus system), at the load scaling factor of 1.0, the system has one high-voltage solution and 9 (or 605) low-voltage solutions. The proposed voltage stability margin index, i.e., the minimum distance in voltage between the high-voltage solution and all low-voltage solutions, is 1.023 (or 1.222). System total load is increased by scaling up all loads proportionally from the default load level to the highest possible load at the nose point over 12 identical steps. At each of these 12 steps, multiple real power flow solutions are solved by HEBC, which are then used for calculating the proposed voltage stability margin indices. As a result, Fig. 6 shows how the proposed voltage stability margin decreases when the load level increases.

It should be noted that the proposed voltage stability margin always reaches zero when the system total load reaches the maximum loading condition at the nose point. This is because the saddle-node bifurcation occurs at the nose point, where the last two real power flow solutions collapse, including a high-voltage solution and a low-voltage solution. Another important observation is that generally speaking, at a lighter loading condition, there are a lot more real power flow solutions. Extensive numerical studies show that the total time cost for HEBC is roughly proportional to the number of real power flow solutions. Therefore, it takes a longer time to calculate the proposed voltage stability margin index at a lighter load level. This is fine as power systems are less likely to have long-term voltage stability issues at a lighter load level. When a power system approaches its nose point, the load level is usually high such that there are fewer real power flow solutions that can be identified by HEBC relatively faster. This is desired because the proposed voltage stability margin index can be evaluated more frequently when the load level and risk of voltage instability are both high.

V. CONCLUSION

The paper solves multiple real power flow solutions for several standard IEEE test cases: Case14, Case30, Case39 and Case57. All investigated solution sets are posted online with this paper. The existence of “short circuit” solutions is pointed out, which represent a set of real power flow solutions that do not satisfy the Kirchhoff Current Law. Numerical techniques to avoid “short circuit” solutions are discussed. The distribution patterns of multiple real power flow solutions are visualized and analyzed. A long-term voltage stability margin index based on multiple real power flow solutions is proposed and numerical studies are conducted to show the feasibility and effectiveness of this index.

In the future, the proposed voltage stability index will be compared with other existing indices to figure out its advantages and disadvantages. In addition, further research for the application of multiple power flow solutions will also be investigated, including (i) the geometric structure of power

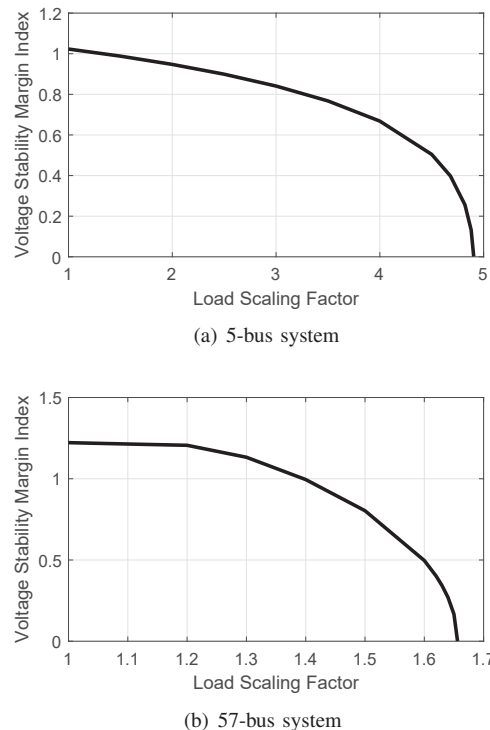


Fig. 6: The proposed voltage stability margin v.s. load increase

balance equations; (ii) advanced computational methods for finding multiple power flow solutions; (iii) applications on transient stability analyses.

REFERENCES

- [1] D. Wu and B. Wang, “Collection of numerous power flow solutions of standard IEEE test systems.” Available at <https://dx.doi.org/10.21227/24bh-hj72>, 2019.
- [2] Q. Hou, E. Du, N. Zhang, and C. Kang, “Impact of high renewable penetration on the power system operation mode: A data-driven approach,” *IEEE Transactions on Power Systems*, vol. 35, no. 1, pp. 731–741, 2020.
- [3] Y. Tamura, Y. Nakanishi, and S. Iwamoto, “Relationship between voltage instability and multiple load flow solutions in electric power systems,” *IEEE Transactions on Power Apparatus and Systems*, vol. PAS-102, pp. 1115–1123, 1983.
- [4] H.-D. Chiang, *Direct methods for stability analysis of electric power systems: theoretical foundation, BCU methodologies, and applications*. John Wiley & Sons, 2011.
- [5] D. Mehta, H. D. Nguyen, and K. Turitsyn, “Numerical polynomial homotopy continuation method to locate all the power flow solutions,” *IET Generation, Transmission & Distribution*, vol. 10, no. 12, pp. 2972–2980, 2016.
- [6] D. Wu and B. Wang, “A holomorphic embedding based continuation-method for identifying multiple power flowsolutions,” *IEEE Access*, accepted, 2019.
- [7] J. Modarresi, E. Gholipour, and A. Khodabakhshian, “A comprehensive review of the voltage stability indices,” *Renewable and Sustainable Energy Reviews*, vol. 63, pp. 1–12, 2016.
- [8] C. DeMarco and T. Overbye, “An energy based security measure for assessing vulnerability to voltage collapse,” *IEEE Transactions on Power Systems*, vol. 5, no. 2, pp. 419–427, 1990.
- [9] T. Overbye and C. DeMarco, “Improved techniques for power system voltage stability assessment using energy methods,” *IEEE Transactions on Power Systems*, vol. 6, no. 4, pp. 1446–1452, 1991.
- [10] F. Milano, *Power System Modelling and Scripting*. Springer, Berlin, Heidelberg, 2010.